Statistical mechanics of dense ionized matter. VI. Electron screening corrections to the thermodynamic properties of the one-component plasma

Serge Galam and Jean-Pierre Hansen
Laboratoire de Physique Théorique des Liquides, Université Pierre et Marie Curie, 4, Place Jussieu, 75230 Paris Cedex 05, France*
(Received 12 February 1976)

The thermodynamic properties of one-component ionic plasmas in a *responding* (polarized) background of fully degenerate electrons are calculated over a wide range of temperatures and densities. The weak and intermediate screening regimes are treated by two complementary methods which take the one-component plasma in a *rigid* background as a starting point. Thermodynamic perturbation theory is used in the weakly screened ionic plasma typical of white-dwarf matter; this leads to simple, analytic expressions for the thermodynamic properties. Relativistic effects in the very dense electron gas are considered explicitly. A variational method, based on the Gibbs-Bogolyubov inequality, and the physical idea of an effective charge reduction of the ions, yields satisfactory results in the intermediate screening regime typical of the deep interior of Jupiter. Our results are in good agreement with the available Monte Carlo data and represent a significant improvement over previous calculations based on a hard-sphere reference system.

I. INTRODUCTION

Under the pressure and temperature conditions characteristic of degenerate stellar matter (e.g., in white dwarfs or the outer layers of neutron stars) and of the interior of the heavy planets, the lighter elements are generally assumed to be completely ionized. The remaining nuclei can, to a good approximation, be considered as point charges, whereas the electrons are strongly degenerate and, in first approximation, play the role of a rigid, uniform background. If nuclei of one element predominate, the physical situation can be reasonably well described by the simple model of the classical one-component plasma (OCP), which may also be relevant for the description of super-dense matter in laser-driven fusion experiments. The thermodynamic properties as well as the static and dynamic correlation functions of the OCP have been accurately determined in a series of recent Monte Carlo[1,2,3] and molecular-dynamics[4] computer "experiments." The equilibrium properties of the OCP depend only on the single dimensionless parameter $\Gamma = \beta(Ze)^2/a$ where Ze is the charge of the ions, $a = (4\pi\rho/3)^{-1/3}$ is the ion-sphere radius ($\rho = N/V$ is the ion number density), and $\beta = 1/k_B T$.

Since the degenerate electrons play the role of the rigid uniform background, the thermodynamic properties (internal energy, pressure, etc.) of the zero-temperature electron gas must be added to the corresponding ionic properties of the OCP. The former depend only on the dimensionless parameter $r_s = a/(a_0 Z^{1/3})$, where a_0 is the electronic Bohr radius ($a_0 = 0.529$ Å). Such a treatment of the electron gas is only valid if the degeneracy condition is satisfied, i.e. $k_B T/\epsilon_F \ll 1$ which can be reexpressed as: $T \ll 6.10^5/r_s^2$. Here ϵ_F stands for the Fermi energy per electron: $\epsilon_F = \hbar^2(3\pi^2\rho Z)^{2/3}/2m$. This condition is well fulfilled in most astrophysical situations. The ions, on the other hand, can be treated classically because of their considerably higher mass.[5]

However, the picture of considering the electron gas as a perfectly rigid and uniform background is generally a very crude approximation. Even a highly degenerate electron gas will be *polarized* by the ionic charge distribution, and the formation of nonuniform electron "clouds" around each ion will modify the ion-ion interaction. Consequently, the bare Coulomb potential between ions must be replaced by an effective screened potential. The importance of electron screening can be qualitatively discussed in terms of the Thomas-Fermi screening length:

$$\lambda_{TF}/a = (\pi/12Z)^{1/3} r_s^{-1/2} . \quad (1)$$

Since in the crude Thomas-Fermi model the screened interionic potential is $v(r) = (Ze)^2 e^{-r/\lambda_{TF}}/r$, it is clear that electron screening is negligible only in the high-density limit ($r_s \to 0$). In a typical white dwarf (density $\simeq 10^6$ g/cm^3 and predominantly helium composition), we find $r_s \simeq 0.015$, and $\lambda_{TF}/a \simeq 4$. In the deep interior of Jupiter (density $\simeq 5$ g/cm^3 and predominantly hydrogen composition), we find $r_s \simeq 0.7$, and $\lambda_{TF}/a \simeq 0.7$. Hence we see that the screening length is of the order of one or a few interionic spacing, which implies a relatively short-ranged effective interaction compared to the bare Coulomb potential.

The aim of the present paper is the calculation of the thermodynamic properties of the ionic one-component plasma in the presence of a *responding* electron background. This is achieved by relating

the properties of the screened ionic plasma to those of the OCP, for which accurate computer data are available, through thermodynamic perturbation theory.[6] The present work differs essentially from previous calculations in the choice of the reference system. While previous workers used the hard-sphere fluid as their reference,[7,8] we have chosen the OCP to be our reference system. This choice will be shown to be both more natural (the screened ionic plasma reduces to the OCP in the limit $r_s \to 0$) and more useful. The weak ($\lambda_{TF} \gg a$) and intermediate ($\lambda_{TF} \simeq a$) screening regimes will be treated on a slightly different footing. The weakly screened ionic plasma will be studied by thermodynamic perturbation theory, in the generalized random-phase approximation (Sec. II). An expansion in powers of a/λ_{TF} will be presented in Sec. III: This expansion yields simple analytic expressions for the corrections to the thermodynamic properties of the ionic plasma in the range $r_s \ll 1$.[9] In that limit, relativistic effects become non-negligible in the electron gas, and these will be considered explicitly.

The intermediate screening regime, on the other hand, will be studied in the framework of a new variational approach, based on the physical idea of an effective charge reduction (Sec. IV). Results based on this approach will be compared to the more usual hard-sphere variational calculations as well as to recent Monte Carlo data[10,11] in Sec. V. The influence of the assumed form of the electron dielectric constant on the thermodynamic properties will also be discussed. The structure factors of the OCP, which are of central importance in our work, are tabulated in the Appendix.

Our calculations are limited to systems of a single ionic species. The extension to two-component systems awaits a detailed study of the corresponding reference system (i.e., the "two-component plasma" in a rigid uniform background) which is presently under way.

II. THERMODYNAMIC PERTURBATION THEORY

Because of the large mass ratio between ions and electrons, the latter react practically *instantaneously* to any variation of the ionic charge density which plays the role of an *external* charge density:

$$\rho_{ext}(\vec{r}) = Ze \sum_{i=1}^{N} \delta(\vec{r} - \vec{r}_i), \tag{2}$$

where the $\vec{r}_i$ ($1 \leq i \leq N$) are the ion positions, and $\rho_{ext}(\vec{r})$ has the following Fourier transform:

$$\tilde{\rho}_{ext}(\vec{k}) = \frac{Ze}{V} \sum_{i=1}^{N} e^{i\vec{k}\cdot\vec{r}_i}. \tag{3}$$

Hence the induced charge density can be related to the external charge density through the *static* dielectric function $\epsilon(k)$ of the electron gas. To leading order in ρ_{ext} (linear response) we have

$$\tilde{\rho}_{ind}(\vec{k}) = [1/\epsilon(k) - 1]\tilde{\rho}_{ext}(\vec{k}). \tag{4}$$

This is the first term in a systematic expansion of $\tilde{\rho}_{ind}(\vec{k})$ in powers of $\tilde{\rho}_{ext}$.[12] The following terms can be expected to be negligible in the high-density limit ($r_s \ll 1$). The second-order term was explicitly considered by Stevenson[8] in the range $r_s \simeq 1$. We have limited ourselves to the linear response term for two reasons. First, inclusion of higher-order terms leads to expressions for the free energy which require a knowledge of the three- and higher-order distribution functions of the reference system; these must then be approximated by superposition or convolution-type approximations, the validity of which is unknown, especially in the case of the OCP. Secondly, our results for $r_s \gtrsim 1$ show that the uncertainties in the dielectric function of the electron gas are such that screening corrections obtained with various dielectric functions in the framework of linear response theory differ already so much, that it seems pointless to include nonlinear terms which depend even more sensitively on the choice of $\epsilon(k)$.

From Poisson's equation the electrostatic potential due to the total charge density is given by

$$\tilde{\varphi}(\vec{k}) = \frac{4\pi Ze}{k^2\epsilon(k)}\tilde{\rho}_{ext}(\vec{k}) = \frac{4\pi Ze}{k^2}\tilde{\rho}_{ext}(\vec{k}) + \frac{4\pi Ze}{k^2}\left(\frac{1}{\epsilon(k)} - 1\right)\tilde{\rho}_{ext}(\vec{k}), \tag{5}$$

where the first term stems from the *external* charge density and the second term from the *induced* charge density. Replacing $\tilde{\rho}_{ext}(\vec{k})$ by $\rho_{\vec{k}}$ for brevity, the Hamiltonian of the system then reads

$$\mathcal{H} = \frac{1}{2V}{\sum_{\vec{k}}}' \frac{4\pi(Ze)^2}{k^2}(\rho_{\vec{k}}\rho_{-\vec{k}} - N) + \frac{1}{2V}{\sum_{\vec{k}}}' \frac{4\pi(Ze)^2}{k^2}\left(\frac{1}{\epsilon(k)} - 1\right)\rho_{\vec{k}}\rho_{-\vec{k}}. \tag{6}$$

The prime in the sums denotes that the term $\vec{k} = 0$ is omitted, to account for the uniform (nonpolarized) background. In the first term N is subtracted from $\rho_{\vec{k}}\rho_{-\vec{k}}$ in order to eliminate the infinite self-energy of the ions. The first term in (6) accounts for the direct ion-ion interaction; it is identical with the Hamiltonian of the unscreened OCP. The second term corresponds to the indirect, or electron-induced, ion-ion interaction, which vanishes

in the limit of zero screening $[\epsilon(k)=1]$; this second term will be treated as a perturbation.

The problem now lies in the choice of the static dielectric constant of the degenerate electron gas. This can be cast in the general form

$$\epsilon(k)=1+\frac{v^{(0)}(k)\pi_0(k)}{1-G(k)\tilde{v}^{(0)}(k)\pi_0(k)}\,, \tag{7}$$

where $\tilde{v}^{(0)}(k)$ is the bare Coulomb potential

$$\tilde{v}^{(0)}(k)=4\pi(Ze)^2/k^2\,, \tag{8}$$

and $\pi_0(k)$ is the polarizability of the free-electron gas, as first calculated by Lindhard.[13] The unknown function $G(k)$ has been determined by several authors through a variety of approximations.

The simplest approximation is to set $G(k)=0$. This is the random-phase approximation, and the corresponding dielectric constant, which we shall refer to as the Lindhard dielectric constant, is exact only in the limit $r_s \to 0$. It is expected to be reasonably accurate in the range $r_s<1$ and will be used extensively in our calculations. Introducing dimensionless wave numbers $q=ak$, the Lindhard dielectric function reads

$$\epsilon(q)=1+(q_{\mathrm{TF}}^2/q^2)f(y)\,, \tag{9}$$

$$f(y)=\frac{1}{2}+\frac{1-y^2}{4y}\ln\left|\frac{1+y}{1-y}\right|\,, \tag{10}$$

where

$$y=q/2q_{\mathrm{F}}\,, \tag{11}$$

$$q_{\mathrm{F}}=ak_{\mathrm{F}}=(9\pi Z/4)^{1/3} \tag{12}$$

is the dimensionless Fermi wave number, and

$$q_{\mathrm{TF}}=a/\lambda_{\mathrm{TF}}=(12Z/\pi)^{1/3}r_s^{1/2} \tag{13}$$

is the dimensionless Thomas-Fermi wave number. The Thomas-Fermi dielectric constant used in Ref. 9 is recovered if $f(y)$ is set equal to 1 for all y.

The factor $G(k)$ appearing in (7) is meant to correct the Lindhard $\epsilon(k)$ for exchange and correlation effects. Since the pioneer work of Hubbard,[14] several attempts have been made to determine $G(k)$ from first principles. One of the most widely used forms is that proposed by Geldart and Vosko.[15] Among the more recent calculations of $G(k)$ are those of Geldart and Taylor[16] and Toigo and Woodruff.[17] We have used these various dielectric functions in the range $r_s \gtrsim 1$, and a comparison will be made in Sec. V.

Finally, in the high-density limit, the degenerate electron gas becomes relativistic. This occurs when

$$\epsilon_{\mathrm{F}} \gtrsim mc^2\,, \tag{14}$$

i.e. when $r_s \lesssim 0.01$.

In that range the screening corrections are expected to be weak and the relativistic counterpart of the Lindhard dielectric function[18] must be used. This will be examined in Sec. III.

We formulate now the perturbation theory for a general $\epsilon(q)$. The expansion will be specialized to specific dielectric functions later on. Henceforth, only dimensionless quantities will be used. In particular we shall use dimensionless Fourier transforms of the type

$$\tilde{\varphi}(q)=4\pi\rho a^3\int_0^\infty \frac{\sin qr}{qr}\,\varphi(r)r^2\,dr$$

$$=3\int_0^\infty \frac{\sin qr}{qr}\,\varphi(r)r^2\,dr\,, \tag{15}$$

where r is in units of a. With this convention the effective (screened) interionic potential in q space, divided by k_BT, is

$$\beta\tilde{v}(q)=3\Gamma/q^2\epsilon(q)\,. \tag{16}$$

The reference potential is

$$\beta\tilde{v}^{(0)}(q)=3\Gamma/q^2\,,$$

and the perturbation potential is

$$\tilde{w}(q)=\beta\tilde{v}(q)-\beta\tilde{v}^{(0)}(q)=\frac{3\Gamma}{q^2}\left(\frac{1}{\epsilon(q)}-1\right)\,. \tag{17}$$

Since $\epsilon(q)\geq 1$ for all q, $\tilde{w}(q)$ is negative definite.

We start out from the familiar exact expression for the excess free energy per ion, involving an integration over a coupling parameter λ:

$$\frac{\beta F}{N}=\frac{\beta F^{(0)}}{N}+\frac{1}{3\pi}\int_0^\infty S^{(0)}(q)\tilde{w}(q)q^2\,dq$$

$$+\frac{1}{3\pi}\int_0^1 d\lambda\int_0^\infty [S(q;\lambda)-S^{(0)}(q)]\tilde{w}(q)q^2\,dq\,, \tag{18}$$

where the superscript (0) will henceforth refer systematically to the reference system (the OCP). $S(q;\lambda)$ is the structure factor for a system of ions interacting through the potential $\beta\tilde{v}^{(0)}(q)+\lambda\tilde{w}(q)$; $S(q;0)\equiv S^{(0)}(q)$. The perturbation potential (17) is clearly long ranged in $\vec{r}$ space. Hence it seems natural to apply to our problem the perturbation techniques developed for such situations.[19-21]

To lowest order, it is assumed that the perturbation potential does not affect the structure factor of the ionic fluid, i.e., $S(q;\lambda)=S^{(0)}(q)$ for all λ. From Eq. (18) we then obtain the following first-order correction to the Helmholtz free energy:

$$\frac{\beta F_1}{N}=\frac{1}{3\pi}\int_0^\infty S^{(0)}(q)\tilde{w}(q)q^2\,dq\,, \tag{19}$$

so that to first order

$$\frac{\beta F^{(1)}}{N} = \frac{\beta F^{(0)}}{N} + \frac{\beta F_1}{N} . \tag{20}$$

The next term in the expansion of the free energy is obtained by making the "generalized" random-phase approximation (RPA)[19] on the structure factor:

$$S(q;\lambda) = \frac{S^{(0)}(q)}{1+\lambda\tilde{w}(q)S^{(0)}(q)} . \tag{21}$$

The corresponding second-order correction to the free energy is obtained by replacing (21) in (18), and integrating over λ:

$$\frac{\beta F_2}{N} = \frac{1}{3\pi}\int_0^\infty \{\ln[1+\tilde{w}(q)S^{(0)}(q)] - \tilde{w}(q)S^{(0)}(q)\}q^2\,dq , \tag{22}$$

$$\frac{\beta F^{(2)}}{N} = \frac{\beta F^{(0)}}{N} + \frac{1}{3\pi}\int_0^\infty \ln[1+\tilde{w}(q)S^{(0)}(q)]\,q^2\,dq . \tag{23}$$

The second-order term corresponds to the summation of all ring diagrams in the generalized cluster expansion of the free energy.[20,21] These ring diagrams are known to be dominant for long-range potentials (cf. the analogy with the familiar Debye-Hückel theory of electrolytes).

Andersen and Chandler[21] have derived a third term in the cluster expansion of the free energy, by summing a still larger class of diagrams. The corresponding expression for the free energy [Eq. (3.17) of Ref. 21] is again expressible in terms of the structure factor of the reference system alone, but this additional term cannot *a priori* be expected to be very useful here (except in the limit of a very weak perturbation, i.e., $r_s \to 0$) since an important feature of the Andersen-Chandler theory is missing in our problem: Because of the absence of an impenetrable (hard sphere) core in the effective ion-ion potential, the expansion cannot be "optimized" by varying the perturbation potential in the unphysical region inside the core. For that reason we have limited the expansion to second order in the present work. However, we have checked that the neglected third term in the expansion is indeed negligible, compared to the two first terms, in the range $r_s \lesssim 0.1$ (see Table I)

From Eq. (19) and (22) it is clear that the approximate expression of the free energy reduces to simple integrals involving the structure factor of the OCP. The radial distribution function is known accurately from the Monte Carlo work[1,2] for many values of Γ in the range $1 \leq \Gamma \leq 160$. The corresponding structure factors have been calculated as outlined in the Appendix. One difficulty in the calculation of $\beta F_2/N$ is immediately apparent: Since $S^{(0)}(q)$ is positive definite and $\tilde{w}(q)$ is negative, it is clear that in the case of a large perturbation, the argument of the logarithm appearing in the integral of Eq. (22) will become negative in a certain range of q values. From (17) this is seen to occur for sufficiently large values of Γ or r_s (i.e., sufficiently strong screening). The situation is illustrated in Fig. 1 which shows the locus of points in the (Γ, r_s) plane where $1 + S^{(0)}(q) \times \tilde{w}(q) = 0$ for the Lindhard dielectric function, $Z = 1$, and the value $q = 4$ which corresponds roughly

TABLE I. Convergence of the perturbation expansion of the free energy $\beta F/N$, the equation of state $\beta P/\rho$, and the internal energy $\beta U/N$, for $r_s = 0.1$, $Z = 1$ and five values of Γ. For each thermodynamic quantity we give the zero-order term (reference system), the first-order term and the RPA term in the first, second, and third lines. In the case of $\beta F/N$ we also list, in a fourth line, the next term in the Andersen-Chandler[21] expansion.

$\Gamma = 2$	$\Gamma = 10$	$\Gamma = 50$	$\Gamma = 100$	$\Gamma = 140$
		$\beta F/N$		
-1.065	-7.109	-40.823	-84.293	-119.381
-0.555×10^{-1}	-0.133	-0.377	-0.640	-0.839
-0.461×10^{-2}	-0.701×10^{-2}	-0.177×10^{-1}	-0.460×10^{-1}	-0.850×10^{-1}
0.960×10^{-4}	0.424×10^{-3}	0.645×10^{-2}	0.145×10^{-1}	-0.338×10^{-1}
		$\beta P/\rho$		
-0.444	-2.663	-14.361	-29.157	-41.031
0.390×10^{-2}	0.147×10^{-1}	0.315×10^{-1}	0.418×10^{-1}	0.446×10^{-1}
0.167×10^{-2}	0.295×10^{-2}	0.547×10^{-2}	0.603×10^{-2}	0.707×10^{-2}
		$\beta U/N$		
-1.332	-7.990	-43.083	-87.473	-123.093
-0.368×10^{-1}	-0.796×10^{-1}	-0.270	-0.500	-0.689
-0.133×10^{-2}	-0.231×10^{-2}	-0.179×10^{-1}	-0.783×10^{-1}	-0.165

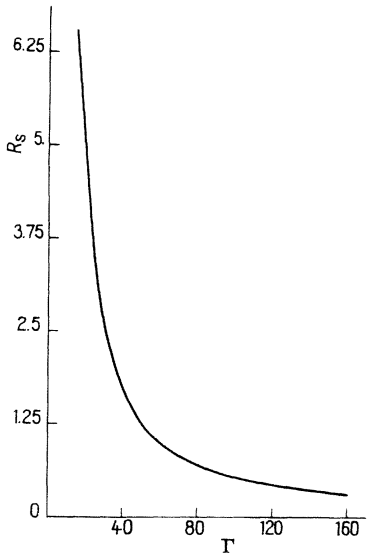

FIG. 1. Range of validity of the generalized RPA.

to the first maximum in the OCP structure factor. All (Γ, r_s) points above the curve yield an imaginary $\beta F_2/N$!

In view of this difficulty (which is a familiar deficiency of the RPA), we have limited our calculations with the perturbation expansion to the range $q_{TF} \lesssim 1$, and the Lindhard dielectric function.

From the free energy, we obtain immediately the excess internal energy and the equation of state through usual thermodynamic relations:

$$\frac{\beta U}{N} = \Gamma \left[\frac{\partial}{\partial \Gamma} \left(\frac{\beta F}{N} \right) \right]_{r_s}, \tag{24}$$

$$\frac{\beta P}{\rho} = \frac{1}{3} \frac{\beta U}{N} - \frac{r_s}{3} \left[\frac{\partial}{\partial r_s} \left(\frac{\beta F}{N} \right) \right]_{\Gamma}, \tag{25}$$

Results from this perturbation theory will be given in Sec. V, and compared to the results obtained by other approaches. We conclude this section by examining the convergence of the perturbation expansion in Tables I and II, for $r_s = 0.1$ and 0.5, and $Z = 1$. The saliant feature is the smallness of the corrections to the thermodynamic properties, compared to the corresponding values for the unperturbed system (the OCP). Except for the lowest values of Γ, the corrections amount only to a few percent of the zero-order term. This feature will be discussed in more detail in Sec. V. At $r_s = 0.1$, the expansion appears to converge very well for the three calculated quantities $\beta F/N$, $\beta U/N$, and $\beta P/\rho$. As expected the situation is much less favorable at $r_s = 0.5$; although the RPA term remains small compared to the first-order term in the expansion of the free energy, it turns out to be of comparable magnitude in the derivatives $\beta U/N$ and $\beta P/\rho$. Moreover the RPA term becomes imaginary for $\Gamma \gtrsim 80$, rendering the expansion useless at large Γ. The situation is even worse for higher values of Z, which imply stronger screening. The perturbation expansion is thus clearly limited to the range $r_s \ll 1$.

III. EXPANSION IN POWERS OF q_{TF}

From (9) and (13) we see that $\epsilon(q) \to 1$ as $q_{TF} \to 0$; the perturbation potential (17) vanishes in that limit. Hence, q_{TF} is a natural "small" expansion parameter in the high-density limit. However, from (19) and (22) it is clear that the corrections to the free energy are rather complicated functions of q_{TF}, and, in particular, are not of a well-defined order in that parameter. Consequently, it seems natural to expand $\beta F_1/N$ and $\beta F_2/N$ in powers of q_{TF}; since the expansion is expected to be valid

TABLE II. Same as in Table I, but for $r_s = 0.5$, without the third term in the Andersen-Chandler expansion of $\beta F/N$.

$\Gamma = 2$	$\Gamma = 10$	$\Gamma = 30$	$\Gamma = 50$	$\Gamma = 70$
		$\beta F/N$		
−1.065	−7.109	−23.710	−40.823	−58.133
−0.207	−0.561	−1.192	−1.739	−2.267
-0.325×10^{-1}	-0.854×10^{-1}	−0.215	−0.427	−0.829
		$\beta P/\rho$		
−0.444	−2.663	−8.477	−14.361	−20.270
-0.254×10^{-2}	0.341×10^{-1}	0.674×10^{-1}	0.934×10^{-1}	0.100
0.555×10^{-2}	0.255×10^{-1}	0.550×10^{-1}	0.702×10^{-1}	0.220×10^{-1}
		$\beta U/N$		
−1.332	−7.990	−25.430	−43.083	−60.811
−0.163	−0.379	−0.871	−1.320	−1.810
-0.240×10^{-1}	-0.563×10^{-1}	−0.246	−0.727	−2.119

only at high densities, we limit ourselves to the case of the Lindhard dielectric function. After a straightforward calculation we obtain

$$\beta F_1/N = -(q_{\mathrm{TF}}^2/\pi)\Gamma I(\Gamma) + \tfrac{1}{6}q_{\mathrm{TF}}^3 + o(q_{\mathrm{TF}}^4), \quad (26)$$

where

$$I(\Gamma) = \int_0^\infty \frac{S^{(0)}(q)f(y)}{q^2}dq, \quad (27)$$

and $f(y)$ is defined through (10) and (11). The integral $I(\Gamma)$ depends only on Γ and can be calculated easily with the help of the OCP structure factors tabulated in the Appendix. The numerical data for $I(\Gamma)$ can be fitted over the range $1 \lesssim \Gamma \lesssim 160$ by the simple expression

$$\Gamma I(\Gamma) = A\Gamma + B\Gamma^{1/4} + C. \quad (28)$$

From a least-squares fit we find for $Z = 1$: $A = 0.057\,93$, $B = 0.971\,12$, $C = -0.343\,11$; for $Z = 2$: $A = 0.110\,20$, $B = 0.786\,38$, $C = -0.132\,31$; for $Z = 6$: $A = 0.166\,01$, $B = 0.861\,49$, $C = -0.209\,25$.

It should be stressed that the integral $I(\Gamma)$, calculated with $f(y) = 1$ (Thomas-Fermi approximation),[9] is independent of Z and differs markedly from the Lindhard results for low values of Z (by a factor of 5 for $Z = 1$ and $\Gamma = 100$!). In fact the Lindhard integral reduces to the Thomas-Fermi result only in the limit $Z \to \infty$, as is immediately clear from Eqs. (9) and (12). For that reason the Thomas-Fermi results of Ref. 9 are only useful in the case of the heavier elements.

In a similiar way, the leading term in the expansion of $\beta F_2/N$ is found to be of order 3 in q_{TF}:

$$\beta F_2/N = -\tfrac{1}{18}q_{\mathrm{TF}}^3 + o(q_{\mathrm{TF}}^4). \quad (29)$$

It is interesting to note that the leading term in $\beta F_2/N$ is one order higher in q_{TF} than the leading term in $\beta F_1/N$, which, *a posteriori*, justifies the labeling of these terms as first- and second-order corrections in the perturbation theory of the free energy. Similarily it can be shown that the third term in the Andersen-Chandler expansion is of order q_{TF}^4. Gathering results, we have

$$\frac{\beta F}{N} = \frac{\beta F^{(0)}}{N} - \frac{q_{\mathrm{TF}}^2}{\pi}\Gamma I(\Gamma) + \frac{q_{\mathrm{TF}}^3}{9} + o(q_{\mathrm{TF}}^4). \quad (30)$$

From (24) and (25) we derive the corresponding expressions for the internal energy and the equation of state:

$$\frac{\beta U}{N} = \frac{\beta U^{(0)}}{N} - \frac{q_{\mathrm{TF}}^2}{\pi}[\Gamma I(\Gamma) + \Gamma^2 I'(\Gamma)] + o(q_{\mathrm{TF}}^4), \quad (31)$$

$$\frac{\beta P}{\rho} = \frac{\beta P^{(0)}}{\rho} - \frac{q_{\mathrm{TF}}^2}{3\pi}\Gamma^2 I'(\Gamma) - \frac{q_{\mathrm{TF}}^3}{18} + o(q_{\mathrm{TF}}^4), \quad (32)$$

where the prime denotes the derivative with respect to Γ. Equations (30), (31), and (32) together with (28) represent simple analytic expressions for the thermodynamic properties of the weakly screened ionic plasma, valid for $q_{\mathrm{TF}} \ll 1$. From (14) it is clear that the dominant correction is linear in r_s, in agreement with the Monte Carlo results of De Witt and Hubbard.[11] The expansion also shows that the corrections to the free and internal energies are negative, while they are positive for the equation of state, except at very low values of Γ.

A difficulty arises in the limit $r_s \to 0$. As pointed out in Sec. II, relativistic effects of the electron gas are expected to become important when $r_s \lesssim 10^{-2}$, which is precisely in the range of white-dwarf matter. The relativistic equivalent of the Lindhard dielectric function has been calculated by Jancovici.[18] Specializing his result to the case of zero frequency, we find $\epsilon(q) = 1 + (q_{\mathrm{TF}}^2/q^2)F(x, y)$, where y is defined by (11), x is the dimensionless relativistic parameter

$$x = \frac{\hbar k_F}{mc} = \frac{1}{137}\left(\frac{9\pi}{4}\right)^{1/3} r_s^{-1}, \quad (33)$$

and the function F is given by

$$F(x, y) = \tfrac{2}{3}(1+x^2)^{1/2} - \frac{2y^2}{3}\sinh^{-1}(x) + (1+x^2)^{1/2}\frac{x^2+1-3x^2y^2}{6yx^2}\ln\left|\frac{1+y}{1-y}\right| + \frac{2y^2x^2-1}{6yx^2}(1+x^2y^2)^{1/2}\ln\left|\frac{y(1+x^2)^{1/2}+(1+x^2y^2)^{1/2}}{y(1+x^2)^{1/2}-(1+x^2y^2)^{1/2}}\right|. \quad (34)$$

In the range $x \lesssim 1$, we expand $F(x, y)$ in powers of x^2:

$$F(x, y) = f(y) + x^2\varphi(y) + o(y^4), \quad (35)$$

where $f(y)$ is the nonrelativistic limit (10), and

$$\varphi(y) = \frac{3}{8}(1-y^2) + \frac{1}{16}\frac{3y^4-4y^2+1}{y}\ln\left|\frac{1+y}{1-y}\right|. \quad (36)$$

To lowest order in q_{TF} we now find

$$\beta F_1/N = -(q_{\mathrm{TF}}^2/\pi)\Gamma I(\Gamma; x) + o(q_{\mathrm{TF}}^3), \quad (37)$$

with

$$I(\Gamma; x) = \int_0^\infty \frac{S^{(0)}(q)F(x; y)}{q^2}dq \quad (38)$$

$$\simeq I(\Gamma) + x^2 J(\Gamma), \quad (39)$$

where

$$J(\Gamma) = \int_0^\infty \frac{S^{(0)}(q)\varphi(y)}{q^2}\, dq\,. \tag{40}$$

We have checked that for $r_s = 0.01$, the error made in replacing (38) by (39) is less than 10% for all Γ values, which is sufficient for our purpose, since the screening corrections are small at such a high density. $\Gamma J(\Gamma)$ can again be fitted over the range $1 \lesssim \Gamma \lesssim 160$ by a simple expression of the form (28) with the following values of the coefficients $Z = 1$: $A = 0.001\,445$, $B = 0.199\,28$, $C = 0.073\,38$; $Z = 2$: $A = 0.003\,562$, $B = 0.384\,10$, $C = -0.094\,67$; $Z = 6$: $A = 0.033\,127$, $B = 0.378\,80$, $C = -0.064\,34$. Expressions for $\beta U/N$ and $\beta P/\rho$, similar to (31) and (32), follow immediately from (37) and (39); it must be kept in mind, in deriving $\beta P/\rho$, that x is a function of r_s [cf. Eq. (33)]. The relativistic effects *increase* the screening corrections by roughly 50% at $r_s = 0.01$, and by less than 10% at $r_s = 0.02$; the increase is somewhat larger for ionic plasmas of higher valence.

IV. VARIATIONAL APPROACH

The perturbation expansion of Sec. II and the related q_{TF} expansion of Sec. III are useful only if $q_{\mathrm{TF}} < 1$. Jovian interior conditions ($r_s \simeq 0.5$, $\Gamma > 10$) on the other hand correspond precisely to the range where the perturbation theory becomes unreliable. For that reason we propose a different approach to deal with the range $q_{\mathrm{TF}} \gtrsim 1$. This is a variational method based on the Gibbs-Bogolyubov inequality:

$$\beta F/N \leq \beta F^{(0)}/N + \beta F_1/N\,, \tag{41}$$

which we use with the OCP as a reference system. Compared to the variational approach based on a reference system of hard spheres, the present method has two major advantages: It becomes exact in the limit $r_s \to 0$, since the screened ionic plasma then reduces to the reference system itself; this means that our variational results can *a priori* be expected to be much more accurate than the hard-sphere results for small values of r_s. Secondly, the comparison in Sec. V will show that the OCP variational free energies are systematically lower than the hard-sphere results even in the range $r_s \gtrsim 1$. Since both sets of data are upper bounds to the exact free energy, our results are necessarily closer to the exact result.

The choice of the variational parameter in the reference system is based on the simple physical picture of charge reduction due to screening: instead of choosing an unscreened reference fluid of ions with charge Ze, as was done in the perturbation theory of Sec. II, it seems reasonable to reduce the charge of the ions to $Z'e$ ($Z' < Z$): $Z'e$ is, roughly speaking, the total charge of an ion and its surrounding electron "cloud." Z' is then the variational parameter in our problem. Since the OCP properties depend only on the dimensionless parameter Γ, the variational parameter will be

$$\Gamma' = (Z'e)^2/ak_BT\,, \tag{42}$$

and the Gibbs-Bogolyubov inequality reads

$$\frac{\beta F(\Gamma; r_s)}{N} \leq \frac{\beta F^{(0)}(\Gamma')}{N} + \frac{\beta F_1(\Gamma'; r_s)}{N}\,. \tag{43}$$

The perturbation potential is now

$$\tilde{w}(q) = \frac{3\Gamma}{q^2}\left(\frac{1}{\epsilon(q)} - \frac{\Gamma'}{\Gamma}\right) = \frac{3\Gamma}{q^2}\left(\frac{1}{\epsilon(q)} - 1\right) + \frac{\Gamma - \Gamma'}{\Gamma'}\,\frac{3\Gamma'}{q^2} \tag{44}$$

instead of (17), so that (43) can be rewritten as

$$\frac{\beta F(\Gamma; r_s)}{N} \leq \frac{\beta F^{(0)}(\Gamma')}{N} + \frac{\Gamma}{\pi}\int_0^\infty S^{(0)}(q; \Gamma')\left(\frac{1}{\epsilon(q)} - 1\right) dq + \frac{\Gamma - \Gamma'}{\Gamma'}\,\frac{\beta U^{(0)}(\Gamma')}{N}\,, \tag{45}$$

where $U^{(0)}$ denotes the excess internal energy of the OCP. For $\beta F^{(0)}/N$ we have used in all our calculations the remarkably simple fit to the Monte Carlo data[2] proposed by De Witt,[22] which is valid in the range $\Gamma \gtrsim 1$:

$$\frac{\beta F^{(0)}}{N} = A\Gamma + B\Gamma^{1/4} + C\ln\Gamma + D\,, \tag{46}$$

where $A = -0.896\,434$, $B = 3.447\,408$, $C = -0.555\,130$, $D = -2.995\,974$. The corresponding $\beta U^{(0)}/N$ is obtained by differentiation with respect to Γ.

Using these expressions and the structure factors of the OCP tabulated in the Appendix, we have minimized the right-hand side of (45) with respect to Γ'. In the range $q_{\mathrm{TF}} \lesssim 1$, we have limited ourselves to the Lindhard dielectric function, whereas for $q_{\mathrm{TF}} > 1$ we have also used the $\epsilon(q)$ of Refs. 15, 16, and 17.

The internal energy and equation of state can be calculated from formulas (24) and (25). Important simplifications occur because of the minimization condition:

$$\frac{\partial}{\partial\Gamma'}\left(\frac{\beta F^{(0)}}{N}(\Gamma') + \frac{\beta F_1}{N}(\Gamma'; r_s)\right) = 0\,. \tag{47}$$

The final formulas are

$$\frac{\beta U(\Gamma; r_s)}{N} = \frac{\Gamma}{\Gamma'}\,\frac{\beta U^{(0)}(\Gamma')}{N} + \frac{\Gamma}{\pi}\int_0^\infty S^{(0)}(q; \Gamma')\left(\frac{1}{\epsilon(q)} - 1\right) dq\,, \tag{48}$$

$$\frac{\beta P(\Gamma; r_s)}{\rho} = \frac{1}{3}\frac{\beta U(\Gamma; r_s)}{N} + \frac{\Gamma}{3\pi}\int_0^\infty S^{(0)}(q;\Gamma') r_s \frac{\partial \epsilon(q)}{\partial r_s}\frac{dq}{\epsilon(q)^2}. \quad (49)$$

The results obtained by the variational method will be presented and discussed in the following section. Here, we only wish to point out that the ratio Γ'/Γ *decreases* as q_{TF} (i.e., r_s or Z) increases (see column 2 of Tables III–V), as one would expect since the effective charge reduction becomes gradually more important with an increase in electron screening. On the other hand for fixed values of q_{TF}, the ratio Γ'/Γ depends only weakly on Γ.

V. RESULTS

This section is devoted to a systematic comparison of the results, obtained by the methods introduced in Sections II–IV, with the existing data of other workers. In a first set of tables we compare our results, obtained variationally or by the perturbation expansion, to the Monte Carlo (MC) data of De Witt and Hubbard[11] and the hard-sphere variational results of Ross and Seale.[7] This comparison is limited to $Z = 1$, $r_s \leq 1$, and the Lindhard dielectric function. In the range $r_s \geq 1$ on the other hand, we compare the results obtained with different dielectric functions.

A few preliminary remarks must be made concerning the hard-sphere calculations of Ross and Seale; their variational parameter is the hard-sphere packing fraction η. However, the free energies which they obtain cannot be considered as true upper bounds to the free energy of the screened ionic plasma for two reasons. First, they use the analytic Percus-Yevick approximation[23] for the structure factor of the hard-sphere fluid to calculate $\beta F_1/N$. This is an excellent approximation for $\eta \lesssim 0.3$; above that value the "exact" structure factors, based on computer simulation results,[24] should be used. We have checked that this modification leads to small, but no entirely negligible corrections to the calculated thermodynamic properties. The second, more serious approximation in the work of Ross and Seale is their modification of the "exact" hard-sphere free energy[25] by an additional term $-\eta$, which has no theoretical justification, but has been added empirically to improve the agreement between the variational and "exact" free energies of a number of fluids.[26] We have repeated the variational calculations without including this empirical modification of the hard-sphere free energy, to obtain an "exact" upper bound to the free energy of the screened ionic fluid. The results obtained with both methods are listed in the tables: heading HS1 refers systematically to our "exact" hard-sphere calculations, whereas HS2 refers to the results obtained by the empirical method of Ross and Seale.

In Tables III–V we compare the thermodynamic properties calculated by the perturbation expansion (Pert.), the q_{TF} expansion, the variational methods based on the OCP (Var. OCP) and the hard-sphere reference systems (Var. HS1 and HS2) to the MC data of De Witt and Hubbard,[11] for $r_s = 0.1$, 0.5, and 1, and $Z = 1$; the Lindhard dielectric function is used throughout. For each value of Γ we have successively listed the deviations $\Delta(\beta F/N)$, $\Delta(\beta P/\rho)$, and $\Delta(\beta U/N)$ of the excess free energy, equation of state, and internal energy from their OCP unscreened values. The results from perturbation theory are listed only under conditions where the RPA term (22) is real. The optimum parameters, Γ' and η_1, which minimize the free energies based on the OCP and hard-sphere variational methods are listed in columns 2 and 3. The unscreened OCP results are listed in column 4. Inspection of the listed results calls for the following remarks:

(i) At $r_s = 0.1$, where the perturbation expansion converges well, it predicts thermodynamic properties in good agreement with the Monte Carlo data and with the OCP variational results. The relative inaccuracy of the MC data is apparent at low values of Γ, where the MC free energies lie *above* the OCP variational results which represent nearly exact upper bounds, since they are based on the very accurate MC data of the unscreened OCP.[2]

(ii) For $r_s = 0.5$ and $r_s = 1$, the perturbation expansion is much less useful, as expected; it converges only for low values of Γ, and predicts free energies which are systematically lower than the MC data and the variational results. As in the case $r_s = 0.1$, the MC free energies lie slightly above the variational results for $\Gamma \lesssim 50$, indicating a small systematic error in the MC results of De Witt and Hubbard; the difference between their *total* free energies and the variational results based on the OCP reference system is less than the estimated error of the MC results (2%) for $\Gamma \gtrsim 5$.

(iii) The variational free energies based on the hard-sphere reference system lie systematically above the variational results based on the OCP. The Ross-Seale empirical modification lowers the free energies somewhat, but their results still lie substantially above the OCP variational free energies. This is not unexpected at $r_s = 0.1$, but remains true even at $r_s = 1$, where the screening corrections to the free energy are important.

TABLE III. Comparison of results of various theories, for $Z=1$ and $r_s=0.1$. For each value of Γ, the first line lists the results for the deviation $\Delta\beta F/N$ of the free energy from its OCP value (which is given in column 4), the second line lists the corresponding deviation $\Delta\beta P/\rho$ of the equation of state, and the third line the deviation $\Delta\beta U/N$ of the internal energy. The Monte Carlo data[11] are listed in column 5, the results of the q_{TF} expansion [Eqs. (30)–(32)] in column 6, the results of the perturbation expansion in column 7, the variational results based on the OCP reference system in column 8, and the variational results based on the hard-sphere reference system in columns 9 and 10. HS1 refers to the "exact" hard-sphere results, and HS2 to the values obtained by the method of Ross and Seale.[7] The optimum values of the variational parameters, Γ' and η_1, are listed in columns 2 and 3. The Lindhard dielectric function is used throughout.

Γ	Γ'	η_1	OCP	Monte Carlo	q_{TF} expansion	Pert.	Var. OCP	Var. HS1	Var. HS2
2	1.710	0.068	−1.065	−0.031	−0.059	−0.060	−0.058	0.225	0.147
			−0.444	0.002	0.007	0.006	0.008	0.106	0.074
			−1.332	−0.026	−0.031	−0.038	−0.028	0.193	−0.110
6	5.400	0.167	−3.972	−0.074	−0.105	−0.105	−0.101	0.450	0.274
			−1.530	0.006	0.014	0.014	0.013	0.144	0.105
			−4.590	−0.055	−0.057	−0.057	−0.055	0.223	0.127
10	9.062	0.220	−7.109	−0.108	−0.139	−0.140	−0.135	0.566	0.338
			−2.663	0.009	0.018	0.018	0.016	0.165	0.125
			−7.990	−0.081	−0.079	−0.082	−0.078	0.237	0.136
20	18.220	0.294	−15.299	−0.183	−0.210	−0.212	−0.206	0.732	0.431
			−5.554	0.014	0.024	0.024	0.022	0.201	0.160
			−16.661	−0.141	−0.130	−0.136	−0.133	0.253	0.149
40	36.420	0.368	−32.232	−0.316	−0.330	−0.338	−0.329	0.899	0.526
			−11.414	0.020	0.032	0.034	0.030	0.245	0.205
			−34.243	−0.257	−0.228	−0.237	−0.230	0.239	0.138
70	63.500	0.425	−58.133	−0.503	−0.494	−0.512	−0.493	1.017	0.589
			−20.270	0.026	0.039	0.039	0.040	0.290	0.252
			−60.811	−0.427	−0.370	−0.408	−0.366	0.187	0.089
100	90.500	0.460	−84.293	−0.684	−0.649	−0.686	−0.646	1.069	0.606
			−29.157	0.030	0.044	0.048	0.047	0.321	0.284
			−87.473	−0.595	−0.510	−0.578	−0.499	0.109	0.014
120	108.260	0.478	−101.815	−0.802	−0.751	−0.803	−0.744	1.082	0.602
			−35.092	0.032	0.047	0.043	0.052	0.336	0.301
			−105.275	−0.706	−0.603	−0.732	−0.583	0.047	−0.046
140	126.200	0.492	−119.381	−0.919	−0.850	−0.924	−0.841	1.083	0.589
			−41.031	0.034	0.049	0.052	0.055	0.350	0.315
			−123.093	−0.817	−0.696	−0.854	−0.670	−0.019	−0.110
160	143.820	0.504	−136.982	−1.036	−0.949	−1.056	−0.936	1.075	0.569
			−46.974	0.036	0.051	0.026	0.060	0.361	0.327
			−140.923	−0.928	−0.788	−1.106	−0.752	−0.091	−0.181

Moreover, the free-energy derivatives ($\Delta\beta P/\rho$ and $\Delta\beta U/N$), calculated with the hard-sphere reference system, differ considerably from the MC data and the OCP variational values.

(iv) The predictions of the expansion in powers of q_{TF} (up to q_{TF}^3) are in surprisingly good agreement with the MC and OCP variational results, even at $r_s=1$ (where $q_{\mathrm{TF}}=1.56$). The agreement for $q_{\mathrm{TF}}>1$ is certainly accidental, and the expansion should only be used in the range $q_{\mathrm{TF}}<1$. In particular, the fact that the q_{TF} expansion predicts a small *negative* correction to the pressure at low Γ and large r_s is probably spurious, since the q_{TF}^3 term in Eq. (32) is then larger than the q_{TF}^2 term.

The most important results of this systematic comparison are summarized in Figs. 2–6.

A similar comparison is made, at $r_s=0.5$, for $Z=2$ and 6 ($q_{\mathrm{TF}}=1.39$ and 2.01, respectively) in Tables VI and VII. No MC data are available for those cases, and the perturbation theory fails since we are in strong screening situations. Hence, we compare only the OCP variational results to their hard-sphere counterparts, in the

TABLE IV. Same as in Table III, but for $r_s = 0.5$.

Γ	Γ'	η_1	OCP	Monte Carlo	q_{TF} expansion	Pert.	Var. OCP	Var. HS1	Var. HS2
2	1.002	0.045	−1.065	−0.158	−0.211	−0.242	−0.235	−0.083	−0.133
			−0.444	0.009	−0.007	0.003	0.017	0.088	0.066
			−1.332	−0.131	−0.157	−0.188	−0.139	−0.007	−0.056
6	3.858	0.121	−3.972	−0.396	−0.443	−0.469	−0.436	−0.119	−0.249
			−1.530	0.031	0.028	0.044	0.039	0.161	0.118
			−4.590	−0.275	−0.283	−0.291	−0.262	−0.073	−0.161
10	6.642	0.170	−7.109	−0.540	−0.613	−0.646	−0.599	−0.177	−0.354
			−2.663	0.046	0.048	0.060	0.051	0.198	0.153
			−7.990	−0.403	−0.393	−0.430	−0.382	−0.157	−0.249
20	13.440	0.240	−15.299	−0.913	−0.966	−1.039	−0.948	−0.345	−0.593
			−5.554	0.069	0.080	0.094	0.074	0.269	0.214
			−16.661	−0.706	−0.650	−0.761	−0.653	−0.347	−0.456
40	26.530	0.315	−32.232	−1.581	−1.567	−1.785	−1.555	−0.719	−1.040
			−11.414	0.099	0.118	0.154	0.109	0.349	0.289
			−34.243	−1.286	−1.138	−1.517	−1.149	−0.761	−0.882
70	45.330	0.375	−58.133	−2.517	−2.386	−3.096	−2.378	−1.310	−1.690
			−20.270	0.127	0.154	0.122	0.150	0.426	0.373
			−60.811	−2.135	−1.850	−3.929	−1.848	−1.395	−1.500
100	63.440	0.412	−84.293	−3.420	−3.164		−3.151	−1.918	−2.334
			−29.157	0.148	0.179		0.185	0.482	0.431
			−87.473	−2.974	−2.551		−2.522	−2.036	−2.135
120	75.200	0.431	−101.815	−4.011	−3.670		−3.649	−2.329	−2.763
			−35.092	0.160	0.193		0.206	0.513	0.462
			−105.275	−3.531	−3.016		−2.962	−2.465	−2.564
140	86.760	0.446	−119.381	−4.597	−4.170		−4.139	−2.742	−3.192
			−41.031	0.170	0.205		0.226	0.539	0.489
			−123.093	−4.086	−3.479		−3.399	−2.897	−2.995
160	98.130	0.459	−136.982	−5.179	−4.664		−4.621	−3.159	−3.621
			−46.974	0.180	0.216		0.245	0.562	0.513
			−140.923	−4.639	−3.940		−3.831	−3.331	−3.428

"exact" (HS1) and Ross-Seale (HS2) versions. Because q_{TF} is significantly larger than one we also list, in the last column of both tables, the OCP variational results based on the Geldart-Vosko[15] dielectric function. For $Z = 2$, the OCP variational free energies still lie significantly below the hard-sphere results, and the pressure corrections calculated by both methods differ considerably.

The influence of the assumed form of the dielectric function on the thermodynamic properties (compare columns 2 and 5) is not negligible. As expected, this influence is even larger at $Z = 6$ (Table VII). In the latter case the deviations of the thermodynamic properties from their OCP values are very large (over 50% on the free and internal energies). The results based on the OCP and hard-sphere systems are in good agreement, but the differences between the results based on the Lindhard and Geldart-Vosko dielectric functions are quite sizeable ($\simeq 10\%$ at high Γ). Note that the screening corrections to the pressure are *negative* in this case.

The influence of the choice of dielectric function is also illustrated by Table VIII, where we compare the corrections to the thermodynamic properties, obtained with three different dielectric functions, at $r_s = 1.5$ and for $Z = 1$. The dielectric function of Toigo and Woodruff[17] is probably the most reliable and we have added, for comparison, the variational results based on the hard-sphere reference system and this same dielectric function (two last columns). It is seen that even at $r_s = 1.5$, the OCP model yields the lowest variational free energies, but the results obtained by both variational methods agree rather closely,

TABLE V. Same as in Table III, but for $r_s = 1$.

Γ	Γ'	η_1	OCP	Monte Carlo	q_{TF} expansion	Pert.	Var. OCP	Var. HS1	Var. HS2
2	0.942	0.033	−1.065	−0.315	−0.297	−0.416	−0.380	−0.300	−0.337
			−0.444	0.017	−0.077	−0.020	0.008	0.061	0.044
			−1.332	−0.263	−0.315	−0.368	−0.252	−0.172	−0.207
6	2.795	0.091	−3.972	−0.739	−0.761	−0.867	−0.787	−0.590	−0.690
			−1.530	0.063	−0.006	0.053	0.040	0.145	0.101
			−4.590	−0.550	−0.566	−0.599	−0.522	−0.385	−0.464
10	4.770	0.131	−7.109	−1.080	−1.102	−1.242	−1.098	−0.835	−0.975
			−2.663	0.091	0.035	0.084	0.066	0.197	0.146
			−7.990	−0.806	−0.786	−0.922	−0.738	−0.581	−0.670
20	9.712	0.196	−15.299	−1.827	−1.807	−2.129	−1.779	−1.386	−1.589
			−5.554	0.138	0.098	0.159	0.100	0.283	0.226
			−16.661	−1.411	−1.300	−1.827	−1.280	−1.058	−1.151
40	18.830	0.265	−32.232	−3.163	−3.011		−2.977	−2.398	−2.670
			−11.414	0.197	0.174		0.154	0.403	0.334
			−34.243	−2.571	−2.277		−2.280	−1.961	−2.070
70	31.260	0.325	−58.133	−5.035	−4.648		−4.616	−3.843	−4.172
			−20.270	0.255	0.245		0.221	0.506	0.444
			−60.811	−4.270	−3.700		−3.697	−3.323	−3.419
100	42.710	0.360	−84.293	−6.840	−6.203		−6.166	−5.250	−5.639
			−29.157	0.297	0.296		0.280	0.599	0.501
			−87.473	−5.949	−5.103		−5.069	−4.644	−4.710
120	50.002	0.379	−101.815	−8.023	−7.216		−7.169	−6.177	−6.561
			−35.092	0.320	0.324		0.315	0.643	0.572
			−105.275	−7.062	−6.032		−5.970	−5.533	−5.664
140	56.850	0.394	−119.381	−9.195	−8.215		−8.156	−7.098	−7.497
			−41.031	0.341	0.348		0.351	0.685	0.613
			−123.093	−8.171	−6.958		−6.858	−6.416	−6.522
160	63.540	0.408	−136.982	−10.358	−9.204		−9.130	−8.013	−8.425
			−46.974	0.360	0.370		0.385	0.721	0.650
			−140.923	−9.279	−7.881		−7.741	−7.300	−7.404

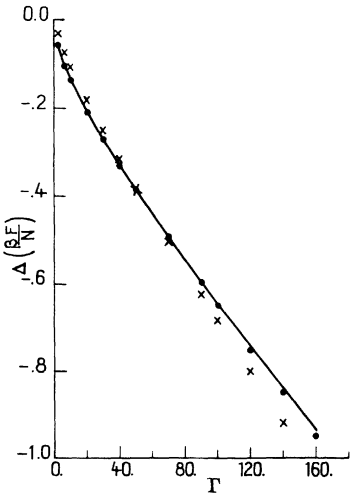

FIG. 2. Deviation of the Helmholtz free energy from the OCP value, as a function of Γ, along the isochore $r_s = 0.1$. Full curve: variational results based on the OCP reference system; dots: expansion (30); crosses: Monte Carlo results (Ref. 11).

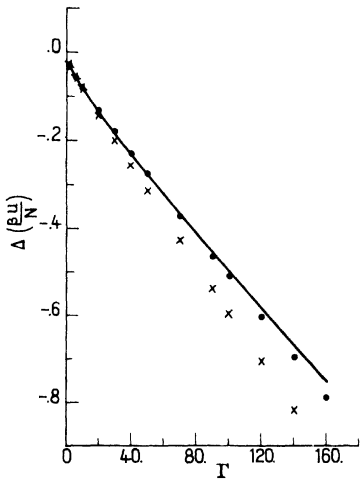

FIG. 3. Same as Fig. 2, but for the deviation of the internal energy.

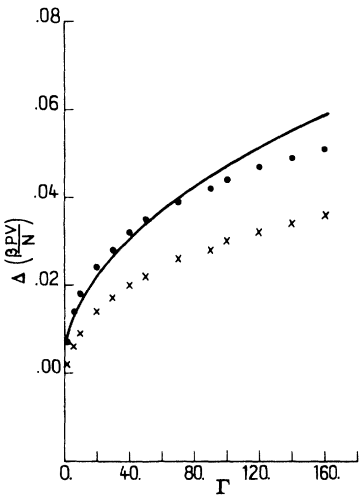

FIG. 4. Same as Fig. 2, but for the deviation of the equation of state.

except for the pressure.

Finally we show in Fig. 7 the corrections to the equation of state, calculated by the OCP variational method, along the isotherm $T = 10^4$ °K for $Z = 1$ (H), which is typical of Jovian interior conditions. Since T is fixed, r_s is inversely proportional to Γ. Three different dielectric functions are used: Lindhard, Geldart-Vosko, and Toigo-Woodruff. The results are seen to differ greatly below $\Gamma \simeq 60$, i.e., $r_s \gtrsim 0.5$. The equation-of-state

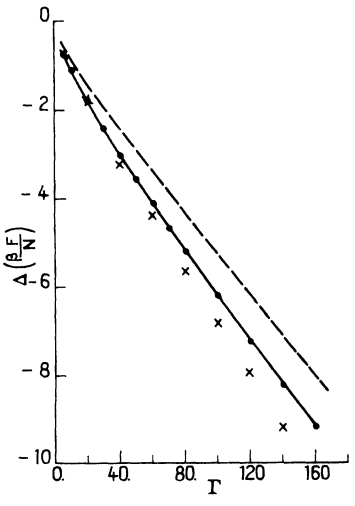

FIG. 5. Deviation of the Helmholtz free energy from the OCP value, as a function of Γ, along the isochore $r_s = 1$. Full curve: OCP variational results; dashed curve: hard-sphere variational results (HS1); dots: expansion (30); crosses: Monte Carlo data (Ref. 11).

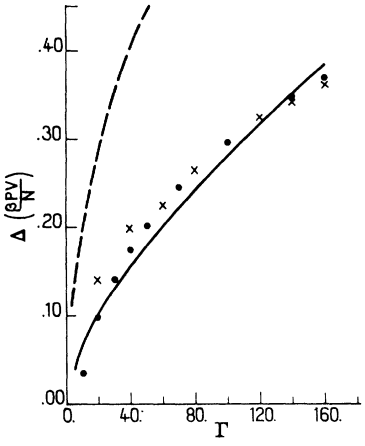

FIG. 6. Same as Fig. 5, but for the equation of state.

corrections, which are considerably smaller than the free- and internal-energy corrections, are the most sensitive to the choice of dielectric function. This is also quite clear from Fig. 8, where we show the variations of $\Delta\beta F/N$, $\Delta\beta U/N$, and $\Delta\beta P/\rho$ as a function of r_s, for a fixed Γ ($\Gamma = 50$), using the Lindhard and Toigo-Woodruff dielectric constants.

VI. DISCUSSION

We have presented detailed calculations of the thermodynamic properties of a one-component ionic plasma in the presence of a responding degenerate electron background, over a wide range of physical conditions. All our calculations have in common the use of the unscreened one-component plasma (OCP) as a reference system.

In the high density or weak screening limit ($q_{TF} < 1$) characteristic of white-dwarf matter, we have derived a simple expansion in powers of q_{TF}. The analytic expressions (30), (31), and (32) for the free and internal energies and the equation of state allow a quick computation of the thermodynamic properties in that limit, for any ionic species, i.e., any value of Z. In the very-high-density range, we have taken care of relativistic effects in the electron gas, by using the relativistic counterpart of the Lindhard dielectric function.

In the intermediate screening range ($q_{TF} \simeq 1$) characteristic of the interior of Jupiter, and possibly of metallic hydrogen, the perturbation theory which leads to the q_{TF} expansion, breaks down, and we have introduced a powerful variational method, using the effective reduced ionic charge as a parameter to minimize the free energy. Our results are in good general agree-

TABLE VI. Variational results for $\Delta\beta F/N$, $\Delta\beta P/\rho$, and $\Delta\beta U/N$, for a helium plasma ($Z=2$) at $r_s=0.5$. In columns 2, 3, and 4 the results of the three variational methods, using the Lindhard dielectric function, are compared. In the last column we list the OCP variational results based on the Hubbard-Geldart-Vosko dielectric function.[15]

Γ	Var. OCP (1)	Var. HS1	Var. HS2	Var. OCP (2)
2	−0.518	−0.456	−0.487	−0.543
	0.000	0.047	0.029	0.006
	−0.371	−0.302	−0.337	−0.390
6	−1.153	−0.987	−1.074	−1.209
	0.018	0.114	0.079	0.036
	−0.855	−0.730	−0.790	−0.893
10	−1.693	−1.451	−1.577	−1.772
	0.030	0.161	0.112	0.056
	−1.293	−1.119	−1.201	−1.345
20	−2.917	−2.528	−2.716	−3.042
	0.038	0.220	0.165	0.081
	−2.353	−2.098	−2.187	−2.440
40	−5.178	−4.578	−4.839	−5.384
	0.048	0.275	0.205	0.117
	−4.388	−4.038	−4.152	−4.543
70	−8.387	−7.593	−7.917	−8.704
	0.062	0.276	0.207	0.169
	−7.342	−7.000	−7.114	−7.592
100	−11.492	−10.593	−10.959	−11.915
	0.076	0.244	0.173	0.219
	−10.240	−9.985	−10.106	−10.582
120	−13.529	−12.592	−12.979	−14.019
	0.084	0.211	0.146	0.252
	−12.153	−11.989	−12.103	−12.557
140	−15.545	−14.592	−14.997	−16.102
	0.093	0.176	0.110	0.285
	−14.057	−13.996	−14.111	−14.520
160	−17.546	−16.594	−17.014	−18.169
	0.102	0.133	0.070	0.317
	−15.952	−16.012	−16.124	−16.475

TABLE VII. Same as in Table VI, but for $Z=6$.

Γ	Var. OCP (1)	Var. HS1	Var. HS2	Var. OCP (2)
2	−1.566	−1.556	−1.567	−1.679
	−0.169	−0.161	−0.167	−0.165
	−1.342	−1.327	−1.337	−1.452
6	−4.043	−4.013	−4.041	−4.362
	−0.384	−0.360	−0.377	−0.280
	−3.535	−3.498	−3.520	−4.380
10	−6.339	−6.285	−6.326	−6.849
	−0.579	−0.542	−0.568	−0.532
	−5.618	−5.560	−5.592	−6.090
20	−11.788	−11.696	−11.767	−12.760
	−1.026	−1.001	−1.045	−0.931
	−10.657	−10.613	−10.665	−11.568
40	−22.218	−22.126	−22.240	−24.077
	−1.923	−1.941	−2.003	−1.679
	−20.563	−20.604	−20.682	−22.284
70	−37.516	−37.441	−37.596	−40.591
	−3.434	−3.349	−3.408	−2.804
	−35.505	−35.483	−35.557	−38.198
100	−52.676	−52.585	−52.765	−56.880
	−4.899	−4.749	−4.815	−4.048
	−50.370	−50.294	−50.372	−54.099
120	−62.733	−62.626	−62.819	−67.699
	−5.859	−5.676	−5.737	−5.171
	−60.244	−60.140	−60.211	−64.890
140	−72.760	−72.636	−72.840	−78.504
	−6.811	−6.602	−6.667	−6.090
	−70.099	−69.974	−70.047	−75.560
160	−82.763	−82.622	−82.835	−89.288
	−7.758	−7.537	−7.595	−6.974
	−79.940	−79.808	−79.870	−86.197

ment with the MC data of De Witt and Hubbard; in particular, they exhibit the linearity of the screening corrections in r_s, up to $r_s \simeq 1$. In the same density range our variational free energies are systematically lower than the results based on the hard-sphere reference system, and the derivatives agree much better with the MC data.

We have extended the calculations to the range $r_s > 1$, where no MC data are yet available. However, at such relatively low densities, the results are very sensitive to the assumed form of the dielectric constant of the electron gas. As is well known, the Lindhard function, which ignores exchange and correlation effects, becomes very inadequate in that range. The results obtained with the widely used Hubbard-Geldart-Vosko function and the more recent Toigo-Woodruff dielectric constant, differ significantly for $r_s > 1$.

To conclude we would like to point out two striking features of our results. First, it is remarkable that the deviations of the calculated thermodynamic properties from their unscreened (OCP) counterpart are relatively small, even in the range where $q_{TF} \simeq 1$. The relative importance of the corrections *decreases* as Γ increases. This can be qualitatively understood by noting that there is a competition between the screening of the ions themselves, characterized by an ionic screening length λ_i, and the screening due to the polarized electron background, which is characterized by the Thomas-Fermi length $\lambda_{TF} = 1/q_{TF}$. For $\Gamma \ll 1$, λ_i is roughly equal to the Debye length

TABLE VIII. Comparison of thermodynamic properties ($\Delta\beta F/N$, $\Delta\beta P/\rho$, $\Delta\beta U/N$) obtained by variationally by for a hydrogen plasma, at $r_s = 1.5$, using three different dielectric functions: Lindhard (1), Hubbard-Geldart-Vosko (2) and Toigo-Woodruff (3). The variational results based on the OCP reference system are listed in columns 5–7; the results obtained by both hard-sphere variational methods (HS1 and HS2) are listed for the Toigo-Woodruff dielectric function only, and should be compared to the data labeled OCP (3). The optimum values of the variational parameters, corresponding to the Toigo-Woodruff dielectric constant, are given in columns 2 and 3.

Γ	Γ'	η_1	OCP	Var. OCP (1)	Var. OCP (2)	Var. OCP (3)	Var. HS1	Var. HS2
2	0.703	0.027	−1.065	−0.506	−0.544	−0.567	−0.388	−0.420
			−0.444	−0.005	0.002	0.007	0.078	0.059
			−1.332	−0.356	−0.385	−0.406	−0.234	−0.269
6	1.750	0.077	−3.972	−1.090	−1.173	−1.231	−0.780	−0.865
			−1.530	0.029	0.054	0.072	0.198	0.155
			−4.590	−0.755	−0.812	−0.859	−0.504	−0.568
10	2.722	0.090	−7.109	−1.554	−1.670	−1.757	−1.633	−1.730
			−2.663	0.059	0.101	0.133	0.241	0.193
			−7.990	−1.086	−1.158	−1.224	−1.158	−1.220
20	5.437	0.136	−15.299	−2.550	−2.724	−2.867	−2.700	−2.843
			−5.554	0.102	0.175	0.236	0.416	0.347
			−16.661	−1.871	−1.970	−2.072	−1.993	−2.069
40	10.752	0.190	−32.232	−4.307	−4.570	−4.808	−4.569	−4.767
			−11.414	0.165	0.275	0.373	0.678	0.591
			−34.243	−3.354	−3.516	−3.696	−3.553	−3.638
70	17.070	0.239	−58.133	−6.723	−7.101	−7.468	−7.136	−7.380
			−20.270	0.259	0.418	0.567	0.966	0.876
			−60.811	−5.461	−5.714	−6.008	−5.813	−5.891
100	22.012	0.268	−84.293	−9.015	−9.497	−9.988	−9.578	−9.852
			−29.157	0.353	0.561	0.760	1.229	1.123
			−87.473	−7.502	−7.838	−8.244	−8.001	−8.086
120	24.812	0.284	−101.815	−10.501	−11.049	−11.621	−11.167	−11.456
			−35.092	0.415	0.656	0.887	1.377	1.270
			−105.275	−8.841	−9.231	−9.711	−9.452	−9.535
140	27.320	0.297	−119.381	−11.964	−12.576	−13.227	−12.733	−13.035
			−41.031	0.478	0.751	1.014	1.519	1.404
			−123.093	−10.168	−10.661	−11.165	−10.892	−10.977
160	29.570	0.308	−136.982	−13.408	−14.082	−14.812	−14.282	−14.595
			−46.974	0.541	0.845	1.140	1.653	1.521
			−140.923	−11.485	−11.980	−12.607	−12.325	−12.419

$\lambda_D = 1/(3\Gamma)^{1/2}$. Electron screening effects will be important, if $\lambda_{TF} < \lambda_D$. For $\Gamma > 1$, the concept of a Debye length loses its significance because of the appearance of short-range order.[1,2] Under these conditions, λ_i is roughly equal to the mean interionic spacing, i.e. $\lambda_i \simeq 1$, and electron screening effects are expected to be important only if $\lambda_{TF} < 1$, i.e. $q_{TF} > 1$.

The second striking feature is the fact that the calculated deviation of the equation of state from its OCP value is consistently smaller, by an order of magnitude, than the corresponding deviations of the free and internal energies, and is of opposite sign, at least as long as $q_{TF} \lesssim 1$. There seems to be no obvious explanation for this systematic behavior.

ACKNOWLEDGMENTS

We are indebted to Bernard Jancovici and Roger Taylor for useful discussions and to Michael Klein for carefully reading the manuscript. One of us (J.P.H.) has greatly benefited from many stimulating conversations with Hugh De Witt, during a very successful visit to the Lawrence Livermore Laboratory. The hospitality of Bill Hoover and the collaboration of Roy Pollock during that visit are also gratefully acknowledged.

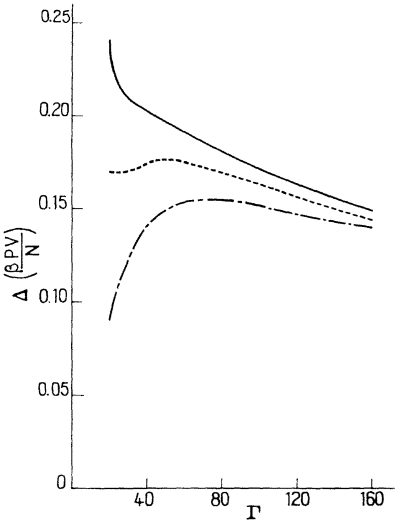

FIG. 7. Deviation of the equation of state of ionic hydrogen from its OCP value, as a function of Γ, along the isotherm $T = 10^4$ °K. The full, dashed, and dash-dotted curves correspond to the Toigo-Woodruff, Hubbard-Geldart-Vosko, and Lindhard dielectric functions. Note that r_s varies with Γ according to $r_s = 31.55/\Gamma$.

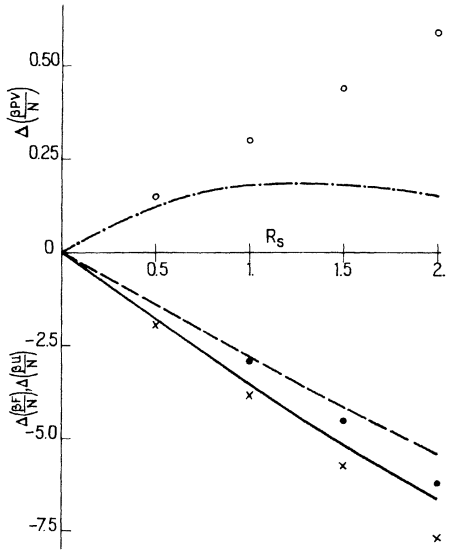

FIG. 8. Deviations of thermodynamic properties of ionic hydrogen from the OCP values, at constant Γ ($\Gamma = 50$), as a function of r_s, calculated by the OCP variational method, using the Lindhard (curves), and Toigo-Woodruff (dots and crosses) dielectric constants. Upper part of graph: $\Delta\beta P/\rho$. Lower part of graph: Helmholtz free energy (full and crosses) and internal energy (dashed curve and full circles). Note the difference in scale above and below the r_s axis.

APPENDIX

Here we give a brief outline of our method for calculating the structure factor of the OCP, starting from the pair-distribution function $g(r)$ obtained by the Monte Carlo simulations of Ref. 2. $S(q)$ is tabulated as a function of q for 9 values of Γ in Table IX. If $x = r/a$ and $q = ak$, the structure factor is derived from $g(r)$ by the Fourier transform:

$$S(q) = 1 + 3\int_0^\infty [g(x) - 1]\frac{\sin kx}{kx}x^2 dx\,. \tag{A1}$$

However, since the simulated systems are of finite size (a few hundred particles in a cubic volume, with periodic boundary conditions) $g(x)$ is determined in the MC calculations only in the range $x \leq \frac{1}{2}L$, where L is the cube edge, which is typically of order 5. At large values of Γ, $g(x)$ has pronounced oscillations which are not yet sufficiently damped for $x = \frac{1}{2}L$, so that large truncation errors occur in the evaluation of (A1). Consequently an extrapolation scheme is needed to obtain accurate values of $g(x)$ in the range $x > \frac{1}{2}L$. Our procedure is inspired by a similar scheme devised by Verlet[27] in the study of simple liquids, and is based on the observation, that the Ornstein-Zernike direct correlation function $c(x)$ approaches rapidly its Debye-Huckel limit

$$c_{\mathrm{DH}}(x) = -\Gamma/x \tag{A2}$$

irrespective of the value of Γ. The MC calculations have shown that $c(x)$ differs from $c_{\mathrm{DH}}(x)$ by less than 1% already at distances of the order of the mean interionic spacing ($x \simeq 1.6$). For $x > \frac{1}{2}L$, the difference between $c(x)$ and its asymptotic form is completely negligible. Consequently, we obtain $g(x)$, for $x > \frac{1}{2}L$, by solving the set of equations:

$$g(x) = g_{\mathrm{MC}}(x)\,, \quad x < \tfrac{1}{2}L \tag{A3}$$

$$c(x) = c_{\mathrm{DH}}(x)\,, \quad x > \tfrac{1}{2}L \tag{A4}$$

supplemented by the Ornstein-Zernike relation between $g(x)$ and $c(x)$:

$$g(x) - 1 = c(x) + \frac{3}{4\pi}\int [g(x') - 1]\, c(|\vec{x} - \vec{x}'|)\, d\vec{x}'\,. \tag{A5}$$

In (A3), $g_{\mathrm{MC}}(x)$ denotes pair-distribution function calculated by the MC method for $x < \frac{1}{2}L$. Equations (A3), (A4), and (A5) form a closed set, which can be solved iteratively like the usual integral equations in the theory of liquids. This was done for about 20 values of Γ in the range $2 \leq \Gamma \leq 160$. The

TABLE IX. Structure factor of the OCP, as a function of $q = ak$, for 9 values of Γ.

$q=ka$	$\Gamma=2$	$\Gamma=6$	$\Gamma=10$	$\Gamma=20$	$\Gamma=40$	$\Gamma=70$	$\Gamma=100$	$\Gamma=130$	$\Gamma=160$
1.0	0.157	0.059	0.036	0.019	0.010	0.005	0.004	0.003	0.002
1.4	0.289	0.122	0.078	0.042	0.021	0.012	0.009	0.007	0.005
1.8	0.437	0.215	0.144	0.081	0.042	0.025	0.018	0.014	0.011
2.2	0.582	0.340	0.245	0.144	0.079	0.047	0.034	0.026	0.021
2.6	0.709	0.498	0.393	0.253	0.151	0.092	0.066	0.052	0.043
3.0	0.809	0.673	0.590	0.439	0.297	0.194	0.143	0.113	0.096
3.2	0.848	0.760	0.702	0.575	0.423	0.293	0.222	0.179	0.153
3.4	0.882	0.839	0.814	0.739	0.604	0.457	0.361	0.298	0.261
3.6	0.909	0.910	0.919	0.920	0.853	0.727	0.616	0.530	0.475
3.8	0.931	0.967	1.007	1.094	1.154	1.141	1.073	0.993	0.929
4.0	0.949	1.010	1.073	1.229	1.438	1.638	1.747	1.803	1.808
4.2	0.963	1.041	1.116	1.303	1.598	1.957	2.260	2.534	2.714
4.4	0.974	1.057	1.136	1.315	1.591	1.908	2.168	2.378	2.537
4.6	0.983	1.066	1.138	1.283	1.474	1.647	1.759	1.809	1.858
4.8	0.989	1.066	1.128	1.229	1.324	1.375	1.386	1.360	1.354
5.0	0.994	1.062	1.110	1.168	1.188	1.163	1.123	1.074	1.048
5.2	0.998	1.056	1.089	1.111	1.080	1.013	0.949	0.897	0.862
5.4	1.000	1.047	1.067	1.061	0.999	0.910	0.836	0.786	0.749
5.6	1.002	1.039	1.047	1.020	0.942	0.843	0.766	0.720	0.682
5.8	1.003	1.031	1.029	0.989	0.903	0.803	0.727	0.686	0.648
6.0	1.004	1.024	1.014	0.966	0.880	0.784	0.715	0.676	0.641
6.4	1.005	1.012	0.994	0.943	0.868	0.797	0.752	0.722	0.698
6.8	1.004	1.004	0.985	0.943	0.894	0.861	0.851	0.838	0.833
7.2	1.004	0.999	0.984	0.957	0.943	0.952	0.975	0.987	1.004
7.6	1.003	0.996	0.986	0.977	0.996	1.039	1.081	1.117	1.145
8.0	1.003	0.995	0.990	0.995	1.032	1.092	1.139	1.186	1.215
8.4	1.002	0.996	0.994	1.006	1.044	1.095	1.130	1.157	1.177
8.8	1.002	0.997	0.997	1.011	1.039	1.064	1.069	1.064	1.061
9.2	1.001	0.998	0.999	1.012	1.026	1.021	1.001	0.979	0.959
9.6	1.001	0.998	1.000	1.009	1.009	0.984	0.955	0.929	0.904
10.0	1.001	0.999	1.001	1.005	0.994	0.964	0.938	0.916	0.898
10.8	1.000	1.000	1.001	1.000	0.998	0.974	0.969	0.972	0.979
11.6	1.000	1.001	1.000	0.999	0.994	1.001	1.017	1.032	1.045
12.4		1.001	1.000	0.998	1.000	1.015	1.026	1.032	1.037
13.2		1.000		0.999	1.004	1.007	1.002	0.996	0.988
14.0		1.000		1.001	1.001	0.996	0.990	0.981	0.975
14.8				1.001	1.000	0.996	0.991	0.993	0.994
15.6				1.000	0.999	0.998	1.002	1.007	1.013
16.4				1.000	0.999	1.001	1.004	1.007	1.008
17.2					1.001	1.002	1.002	1.000	0.997
18.0					1.001	1.000	0.999	0.996	0.995
18.8					0.999	0.999	0.998	0.999	0.998
19.6					1.000	1.000	1.000	1.001	1.002
20.4					1.000	1.000	1.000	1.001	1.002

results obtained by this procedure are considerably more accurate than the original data, tabulated in Ref. 2, which were based on a direct evaluation of the statistical average:

$$S(q) = (1/N)\langle \rho_{\vec{q}}\, \rho_{-\vec{q}} \rangle \ , \tag{A6}$$

where $\rho_{\vec{q}}$ is defined by (3). For $q \lesssim 1$, the calculated values of $S(q)$ are indistinguishable from their exact long-wavelength limit[28]:

$$S(q) = \frac{1}{3\Gamma/q^2 + \chi_T^0/\chi_T} \ , \tag{A7}$$

where χ_T^0/χ_T is the ratio of the ideal-gas compressibility over the compressibility of the OCP, which can be easily calculated by taking the second derivative of (46) with respect to Γ. Consequently, we have omitted the low-q values of the structure factors in Table IX. Finally, for $\Gamma \lesssim 1$, $S(q)$ can be calculated quite accurately by solving the HNC integral equation.[29]

*Equipe associée au Centre National de la Recherche Sciéntifique.
[1]S. G. Brush, H. L. Sahlin, and E. Teller, J. Chem. Phys. 45, 2102 (1966).
[2]J. P. Hansen, Phys. Rev. A 8, 3096 (1973).
[3]E. L. Pollock and J. P. Hansen, Phys. Rev. A 8, 3110 (1973).
[4]J. P. Hansen, I. R. McDonald, and E. L. Pollock, Phys. Rev. A 11, 1025 (1975).
[5]J. P. Hansen and P. Vieillefosse, Phys. Lett. 53A, 187 (1975).
[6]R. W. Zwanzig, J. Chem. Phys. 22, 1420 (1954).
[7]M. Ross and D. Seale, Phys. Rev. A 9, 396 (1974).
[8]D. J. Stevenson, Phys. Rev. B 12, 3999 (1975).
[9]J. P. Hansen, J. Phys. (Paris) 36, L133 (1975).
[10]W. B. Hubbard and W. L. Slattery, Astrophys. J. 168, 131 (1971).
[11]H. E. De Witt and W. B. Hubbard (unpublished).
[12]J. Hammerberg and N. W. Ashcroft, Phys. Rev. B 9, 409 (1974).
[13]J. Lindhard, K. Dan. Vidensk. Selsk. Mat.-Fys. Medd. 28, No. 8 (1954).
[14]J. Hubbard. Proc. R. Soc. Lond. A 243, 336 (1957).
[15]D. J. W. Geldart and S. H. Vosko, Can. J. Phys. 44, 2137 (1966).
[16]D. J. W. Geldart and R. Taylor, Can. J. Phys. 48, 167 (1970).
[17]F. Toigo and T. O. Woodruff, Phys. Rev. B 2, 3958 (1970).
[18]B. Jancovicí, Nuovo Cimento 25, 428 (1962).
[19]A. A. Broyles, H. L. Sahlin, and D. D. Carley, Phys. Rev. Lett. 10, 319 (1963); F. Lado, Phys. Rev. 135, A1013 (1964).
[20]P. C. Hemmer, J. Math. Phys. 5, 75 (1964); J. L. Lebowitz, G. Stell, and S. Baer, J. Math. Phys. 6, 1282 (1965).
[21]H. C. Andersen and D. Chandler, J. Chem. Phys. 57, 1918 (1972); H. C. Andersen, D. Chandler, and J. D. Weeks, J. Chem. Phys. 57, 2626 (1972).
[22]H. E. De Witt (unpublished).
[23]M. S. Wertheim, J. Math. Phys. 5, 643 (1964).
[24]L. Verlet and J. J. Weis, Phys. Rev. A 5, 939 (1972).
[25]N. F. Carnahan and K. E. Starling, J. Chem. Phys. 51, 635 (1969).
[26]M. Ross, Phys. Rev. A 8, 1466 (1973).
[27]L. Verlet, Phys. Rev. 165, 201 (1968).
[28]P. Vieillefosse and J. P. Hansen, Phys. Rev. A 12, 1106 (1975).
[29]J. F. Springer, M. A. Pokrant, and F. A. Stevens, J. Chem. Phys. 58, 4863 (1973).